

pubs.acs.org/JACS Article

Metal-Free Heterogeneous Asymmetric Hydrogenation of Olefins Promoted by Chiral Frustrated Lewis Pair Framework

Yin Zhang,[#] Jun Guo,[#] Peter VanNatta, Yao Jiang, Joshua Phipps, Roknuzzaman Roknuzzaman, Hassan Rabaâ, Kui Tan, Thamraa AlShahrani, and Shengqian Ma*



Cite This: J. Am. Chem. Soc. 2024, 146, 979-987



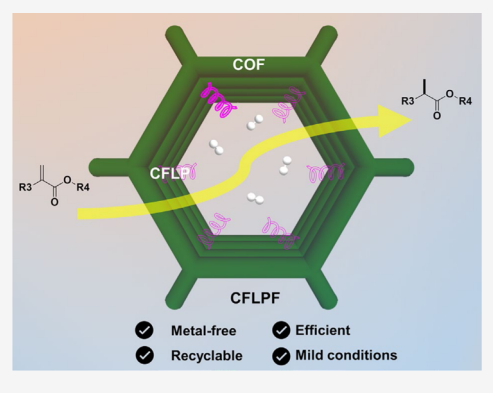
ACCESS I

III Metrics & More

Article Recommendations

Supporting Information

ABSTRACT: The development of metal-free and recyclable catalysts for significant yet challenging transformations of naturally abundant feedstocks has long been sought after. In this work, we contribute a general strategy of combining the rationally designed crystalline covalent organic framework (COF) with a newly developed chiral frustrated Lewis pair (CFLP) to afford chiral frustrated Lewis pair framework (CFLPF), which can efficiently promote the asymmetric olefin hydrogenation in a heterogeneous manner, outperforming the homogeneous CFLP counterpart. Notably, the metal-free CFLPF exhibits superior activity/enantioselectivity in addition to excellent stability/recyclability. A series of in situ spectroscopic studies, kinetic isotope effect measurements, and density-functional theory computational calculations were also performed to gain an insightful understanding of the superior asymmetric hydrogenation catalysis performances of CFLPF. Our work not only increases the versatility of catalysts for asymmetric



catalysis but also broadens the reactivity of porous organic materials with the addition of frustrated Lewis pair (FLP) chemistry, thereby suggesting a new approach for practical and substantial transformations through the advancement of novel catalysts from both concept and design perspectives.

INTRODUCTION

Asymmetric catalysis plays an important role in synthesizing bioactive products that are closely related to human health. In its current state, the performance of existing catalysts remains far from satisfactory, and opportunity for discovery abounds. One specific direction is asymmetric olefin hydrogenation, which represents a class of step-economical and important transformations that flourish in homogeneous catalysis with the cooperation of many metals and delicate chiral ligands.¹ The past decades have witnessed the development of catalysts evolving from expensive noble metals (Rh, Ir, Ru, Pd, etc.)² to earth-abundant transition metals (Ni, Co, Ti, etc.), as well as the advancement of chiral ligands and scaffolds from cyclohexyl(2-methoxyphenyl)methylphosphine (CAMP)⁴ to 2,2'-bis(diphenylphosphino)-1,1'-binaphthyl (BINAP)⁵ and those with 9,9'-spirobifluorene backbone (SFDP),6 etc. All of these efforts have contributed to the improvement of reaction efficiency, productivity, selectivity, and substrate scope for asymmetric olefin hydrogenation. Despite the significant progress, there remain several issues including addressing the poor compatibility of metal complexes, the requisite addition of highly active organolithium reagents in conjunction with a transition metal, and the difficulty in unique chiral ligand synthesis. To alleviate these issues, current efforts are devoted toward two solutions: (1) developing a metal-free catalyst⁷ that may conceptually reduce the sensitivity, toxicity, and cost of metal complexes and (2) constructing a recyclable catalyst that circumvents continuous consumption and repetitive synthesis of chiral ligands. Despite some progress in each aspect, the desired goal of preparing the optimal catalyst showcasing both metal-free and recyclable merits for practical production remains unaddressed.

Recently, the discovery and development of frustrated Lewis pair (FLP) chemistry has unveiled a new dimension in catalysis with the realization of metal-free hydrogenation under mild conditions. Particularly, the coupling of a bulky Lewis base (P/N compounds) with a bulky Lewis acid (B compounds) results in strong steric hindrance that enables the activation of small molecules and C-H bonds among others. This catalytic activity has led to the rapid success of FLP chemistry over the past decade. In a mark of progress, the synthesis and application of chiral frustrated Lewis pairs (CFLPs) have also been realized, performing efficient asymmetric conversions including hydrogenation. The utilization of CFLPs for asymmetric hydrogenation of olefins remains a significant

Received: October 18, 2023 Revised: November 29, 2023 Accepted: November 30, 2023 Published: December 20, 2023





challenge, as achieving simultaneous high reactivity and enantioselectivity is difficult. Moreover, the further prospect of utilizing CFLPs for practical transformations has been hindered since molecular CFLPs bear the same intrinsic drawbacks of all homogeneous catalysts with no/poor reusability and inefficiency in product-catalyst separation.

The development of heterogeneous catalysts for asymmetric hydrogenation is steadily advancing toward the exploration of metal-free catalysts. The construction of privileged chiral ligands into metal-free porous organic materials 12 has shown benefits for scalable production and could avoid the drawback of the chiral molecular catalysts leaching into solution. Nonetheless, these heterogeneous supports have been reported to drive asymmetric olefin hydrogenation only after the introduction of a noble metal complex/nanoparticle, 13 without which the pristine metal-free polymers/crystalline organic frameworks were reported to merely have the capacity for limited catalytic ability within well-investigated reactions such as the Henry, aldol, and Diels-Alder reactions. Therefore, the development of metal-free catalysts based on organic materials for asymmetric olefin hydrogenation is highly desirable, as it may not only enhance the catalyst by eliminating the usage of noble metals but also expand the reactivity of porous organic materials.

In this context, we envision that the conceptually innovative combination of CFLPs with porous organic materials (such as covalent organic frameworks (COFs)) can accomplish two goals with one strategy, as it may simultaneously achieve the development of a catalyst with the capacity for asymmetric olefin hydrogenation and allow for the advancement of porous organic materials based on FLP chemistry. COFs represent a new class of supports because of their robust crystalline structure, tunable metal-free composition and porosity, and superior catalysis compatibility. 14 To the best of our knowledge, the construction of CFLPs in the structure of COFs has not been reported thus far, predominantly due to the difficulty in identifying reactive CFLPs suitable for such a task and a feasible construction strategy to introduce them into COFs. Herein, we demonstrate the postmodification of a rationally designed COF with a newly devised CFLP can realize the development of a new class of metal-free and recyclable catalyst: chiral frustrated Lewis pair framework (CFLPF, Figure 1), which catalyzes asymmetric olefin hydrogenation with excellent activity and enantioselectivity while acting as an indispensable role in advancing both

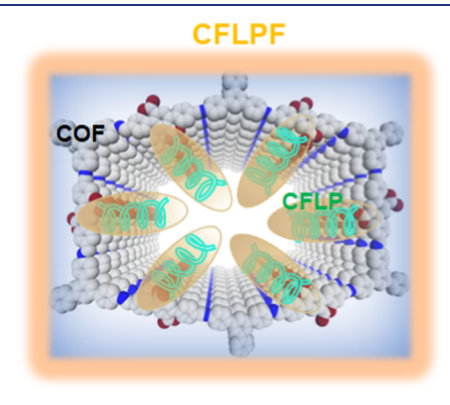


Figure 1. Innovative combination of COF and CFLP for generating a metal-free heterogeneous catalyst CFLPF.

asymmetric olefin hydrogenation and porous organic materials by virtue of FLPs chemistry.

RESULTS AND DISCUSSION

To construct a CFLPF, design considerations are needed from the aspects of both CFLPs and COFs. In particular, the discovery and application of CFLPs are still in their infancy¹¹ and lack a prototype for molecular-level modification. To date, three strategies have been established to create molecular CFLPs: (i) intramolecular CFLPs, (ii) bulky chiral Lewis acid paired with bulky achiral Lewis base, and (iii) coupling bulky achiral Lewis acid with bulky chiral Lewis base. 15 In this work, we aim to employ the third strategy, as there are plentiful chiral Lewis bases that can facilitate access to a new array of CFLPs. We propose that the introduction of bulky chiral Lewis bases into COF functionalized with carboxylate groups is achievable by amidation/esterification of bulky chiral amine/chiral oxazoline which is synthetically available with amino/ hydroxylic derivatives, respectively; the subsequent incorporation of a Lewis acid such as tris(pentafluorophenyl)borane into COF may allow for the successful preparation of CFLPF. To achieve this, a large pore size that can accommodate the bulky CFLPs is required for the carboxylate functionalized COF, which herein was designed and prepared using 1,3,5-tri-(4-aminophenyl)benzene (TAPB) and p-terphenyl-2',5'-dicarboxylic acid-4,4"-dicarboxaldehyde (3P-COOH) (Figure 2). The large pore size of COF-TAPB-3P-COOH was obtained under solvothermal conditions using glacial acetic acid as a catalyst. The crystallinity of the resulting COF was confirmed by the powder X-ray diffraction (PXRD) pattern, which corresponds well with the simulated pattern showing four characteristic peaks assigned to (200), (002), (400), and (004) facets, respectively (Figure S1). The composition of COF-TAPB-3P-COOH was determined as an order combination of TAPB and 3P-COOH by Fourier-transform infrared spectroscopy (FT-IR), displaying the characteristic C=NH vibration at 1688 cm⁻¹ and the disappearance of characteristic -NH₂ double peaks of TAPB (Figure S2). Furthermore, solid-state cross-polarization magic angle spinning carbon-13 nuclear magnetic resonance (CP/MAS ¹³C NMR) clearly revealed the presence of a benzene ring, C=N, and carboxylic group in COF-TAPB-3P-COOH (Figure S3). These results indicate the successful construction of COF via the imine bond formation.

The porous nature of COF-TAPB-3P-COOH was examined by N₂ sorption at 77 K, with a Brunauer-Emmett-Teller (BET) surface area of 691 m²/g and a pore size distribution centered at 2.95 nm (Figure S4), which is large enough to accommodate CFLP moieties. Thereafter, the introduction of freshly synthesized chiral N¹,N¹-di-tert-butyl-3,3-dimethylbutane-1,2-diamine (R1*NH₂) and chiral 4,5-dihydro-4-phenyl-2-oxazolemethanol (R2*OH) as chiral Lewis bases were conducted to yield COF-TAPB-3P-COHNR1* by amination and COF-TAPB-3P-COOR2* by esterification, which was further associated with B(C₆F₅)₃ to afford the target catalysts, defined as CFLPF1 and CFLPF2 (Figure 3), respectively. The process of CFLP introduction into the COF was monitored by FT-IR and displayed the characteristic stretching vibration of C=O (1654 cm⁻¹), bending vibration (1517 cm⁻¹) and stretching vibration (3340 cm⁻¹) of amide N-H, and aliphatic C-H (2960 cm⁻¹) in COF-TAPB-3P-COHNR1*. Additionally, the characteristic stretching vibrations of C=O (1695 cm⁻¹), and aromatic and aliphatic C-H (3030-2926 cm⁻¹) in COF-TAPB-3P-COOR2* were also observed, thus validating

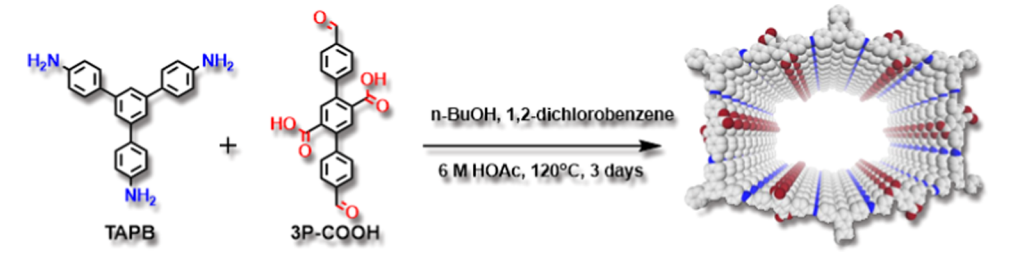


Figure 2. Preparation of COF-TAPB-3P-COOH.

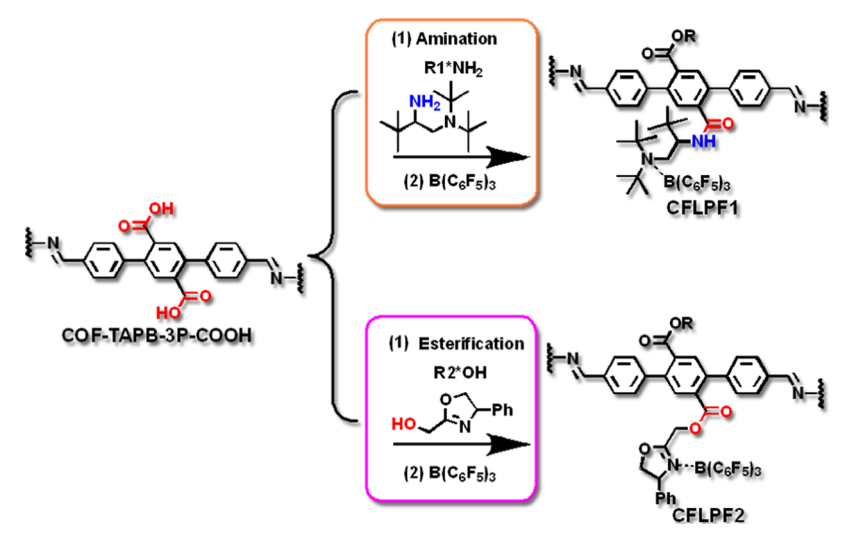


Figure 3. Procedure of preparing CFLPFs.

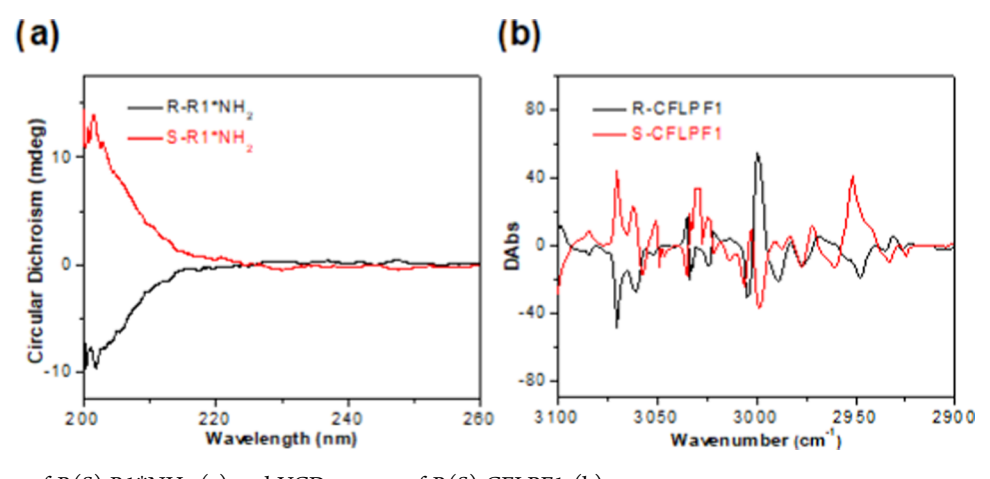


Figure 4. CD spectra of R(S)-R1*NH₂ (a) and VCD spectra of R(S)-CFLPF1 (b).

the successful introduction of chiral Lewis bases by post-modification (Figure S5). The diminished C=O signal of COOH in both cases also implies successful anchoring of CLPFs to COFs. Furthermore, the characteristic C-F vibration in both CFLPF1 and CFLPF2 corroborated the successful incorporation of B(C₆F₅)₃ (Figures S6 and S7). The crystallinity was retained after the addition of CFLP inside the parent COF as revealed by the PXRD patterns of CFLPF1 and CFLPF2 (Figure S8). N₂ sorption isotherms indicated that, after the incorporation of CFLP into COF, the BET surface area decreased in the resulting CFLPF1 (247 m²/g, Figure S9) and CFLPF2 (183 m²/g, Figure S10), whereas the pore size of both samples was distributed in the range of 1.5–3.0 nm, indicative of adequate accessible pores for the ingress of

reactants and egress of products. The morphology of CFLPFs was observed by scanning electronic microscopy (Figure S11) and retained the same morphology of aggregated crystalline particles inherited from COF-TAPB-3P-COOH. The energy-dispersive spectrometry (EDS) mapping showed the order distribution of C, N, and O in COF-TAPB-3P-COOH (Figure S12), and C, N, O, B, and F in CFLPFs (Figures S13 and S14), verifying the successful incorporation of CFLPs into COF at a molecular scale. Diagnostic fluorine signals were observed in the X-ray photoelectron spectroscopy (XPS) surveys of CFLPFs compared with the parent COFs (Figure S15), further supporting the successful introduction of CFLP inside the COF. ¹⁶

To verify the enantiomeric nature of chiral Lewis bases and the corresponding CFLPFs, we performed circular dichroism (CD) and vibrational circular dichroism (VCD) spectroscopy measurements. The synthesized chiral (R and S) R1*NH₂ (Figures 4a and S16) and R2*OH (Figure S17) enantiomers show good chiral purity as they exhibited mirror images of each other in the CD spectra owing to the Cotton effect. Accordingly, CFLPF1 (Figure 4b) and CFLPF2 (Figure S18) displayed mirror images between the R and S enantiomers in the VCD spectra indicative of their excellent chiral induction properties, which result from the dissimilar discrimination capacity toward circularly polarized light of CFLPF1's and CFLPF2's C—H stretching vibrations in the investigated range.

The obtained catalysts' performances were examined in the context of asymmetric hydrogenation of olefins with the isolated yields and enantiomeric excess (ee) values summarized in Table 1 and Figure 5. Unless otherwise stated, the

Table 1. Optimization of Asymmetric Olefin Hydrogenation with CFLPF

entry	catalyst	solvent	yield (%)	ee value (%)
1 ^a	COF	toluene	0	0
2	CFLP1	toluene	75	78
3	CFLP2	toluene	0	0
4	CFLPF1	toluene	95	86
5	CFLP1 + COF	toluene	73	79
6	CFLPF2	toluene	80	0
7^{b}	CFLPF2	toluene	82	63
8 ^c	CFLPF1	toluene	94	-85
9	CFLPF1	CH_2Cl_2	76	65
10	CFLPF1	THF	96	52

"Unless otherwise stated, the reaction proceeded under the following conditions: 2 mL dry solvent, 10 mg catalyst, 0.1 mmol substrate, 60 bar H₂, 48 h at room temperature. The yield was determined by the mass of the isolated product, and the ee value was determined by high-performance liquid chromatography (HPLC). The corresponding NMR spectroscopy and HPLC results of products are provided in the Supporting Information. ^b1-Phenyl-1-aminomethylethene substrate. ^cS-CFLPF1 catalyst.

tested chiral catalysts were R enantiomers. COF-TAPB-3P-COOH did not initiate the transformation of methyl 2-phenyl acrylate (substrate 1a) to the desired product 2a because of its inactivity for hydrogenation (Entry 1). The homogeneous CFLP R1*NH₂ + B(C_6F_5)₃ catalyst afforded moderate yield (75%) and ee value (78%), but was not recyclable (Entry 2). In contrast, although chiral oxazoline Lewis bases have recently been reported to be effective for asymmetric hydrogenation of aldehyde, 15 the homogeneous CFLP R2*OH + B(C₆F₅)₃ was not active toward olefin hydrogenation (Entry 3). This was likely caused by the self-deactivation via the reaction between -OH and B(C_6F_5)₃. ¹⁷ To our delight, CFLPF1 demonstrated a notably high yield (95%) and ee value (86%) (Entry 4). This enhancement compared with the molecular R1*NH2 + $B(C_6F_5)_3$ can be attributed to a higher local concentration of CFLP active sites and the enforced stronger chiral environment within the nanospace of the COF. 18 By contrast, the physical mixture of homogeneous CFLP1 R1*NH₂ + B(C_6F_5)₃

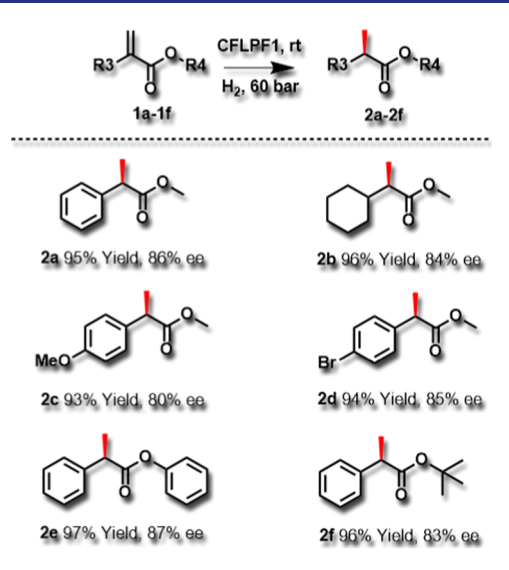


Figure 5. Performance of CFLPF1 in the transformation of different substrates.

and COF-TAPB-3P-COOH could only attain 73% yield and 79% ee (Entry 5) value comparable to that of homogeneous CFLP1, suggesting the importance of synergy within an ordered structure resembling enzymatic catalysis.¹⁹

Surprisingly, CFLPF2, which circumvents the self-deactivation issue in $R_2*OH + B(C_6F_5)_3$, produced a racemic product, albeit in an 80% yield (Entry 6). The striking difference in performance between CFLPF1 and CFLPF2 implies there should exist some specific interaction with the substrate molecule in the vicinity of the active center important for chiral induction, and we hypothesize that hydrogen bonding may serve such a critical role in facilitating the chirality transfer from the catalyst to the substrate. To verify our hypothesis, 1phenyl-1-aminomethylethene, which has the potential to form a hydrogen bond with CFLPF2, was used as the substrate for asymmetric hydrogenation. As anticipated, a successful chirality transfer with a 63% ee value was observed (Entry 7). Meanwhile, the S enantiomer of CFLPF1 exhibited a similar yield (94%) but inverse enantioselectivity (-85%), thus indicating the general chiral induction of CFLPF1 (Entry 8). The influence of solvent on the catalysis performance of CFLPF1 was also assessed, showing that toluene was the best to achieve both a high yield and an ee value among all tested solvents (toluene, CH₂Cl₂, and tetrahydrofuran (THF)). A much lower yield (76%) and ee value (65%) were observed with CH₂Cl₂ (Entry 9), likely due to its poor solubility for substrates, thus hindering the mass transfer. Although a comparable yield (96%) could be obtained with THF as the solvent, a lower ee value (52%) was attained (Entry 10). This can be attributed to (1) THF + $B(C_6F_5)_3$ forming an achiral FLP that is hydrogenation active²⁰ and (2) hydrogen bonding inhibition of THF that is detrimental to chirality transfer.

Recyclability is an important aspect of catalysis for practical application. CFLPF1 showed no obvious decrease in catalysis performance after being used five consecutive times (Figure S19) and retained its structural integrity, composition, and porosity as evidenced by the PXRD (Figure S20), EDS mapping (Figure S21), XPS survey (Figure S22), and BET surface area measurements (Figure S23). Collectively, this verifies its heterogeneous nature with good reusability/recyclability. To quantify the CFLP amount in CFLPF1, the

amount of Lewis acid before and after the recycle test was calculated using nuclear magnetic resonance (NMR) spectroscopy and was determined to be 1.4 mmol per gram of COFTAPB-3P-COOH (Figure S24), indicating no noticeable leaching of CFLP during the reaction process.

These results demonstrate that CFLPFs are excellent in catalytic performance for the asymmetric hydrogenation of olefins. Specifically, the inheritance of crystallinity and porosity from COF allows for the creation of plentiful nanoreactors within which the enriched CFLP boosts asymmetric hydrogenation due to the high local concentration of active sites and the enhanced chiral induction environment. As such, CFLPFs, as a new group of metal-free and recyclable chiral catalysts, will promote further enthusiasm for constructing diverse catalysts and resolving issues not limited to asymmetric hydrogenation.

In view of its superior catalysis performance, CFLPF1 was adopted to expand the substrate scope by catalyzing the asymmetric hydrogenation of different olefins (Figure 5) under the obtained optimal conditions. The olefin with aliphatic substitution (substrate 1b) was readily transformed with a 96% yield and an 84% ee value. Compatible yield (93%) and ee value (80%) were obtained for the substrate with an electrondonating group on the aromatic substitution (substrate 1c). The substrate with halogen on aromatic substitution (substrate 1d) was transformed to the target product with a 94% yield and 85% ee value. In addition, substrate 1e with aromatic ester was also well converted with a yield of 97% and an ee value of 87%. Furthermore, substrate 1f including additional steric hindrance from the t-butyl group was subject to this transformation as well, with a yield of 96% and an ee value of 83%. These results highlight CFLPF1 as an excellent heterogeneous catalyst for the asymmetric hydrogenation of olefins.

Encouraged by the enhanced hydrogenation enantioselectivity by CFLPF1 relative to the homogeneous FLP counterpart, we sought further experimental and computational insights into the catalytic mechanism. First, to probe the direct interaction between H₂ and CFLPF1, we conducted in situ IR measurements with the dry sample upon exposure to gaseous H₂. Figure 6 clearly shows that H₂ is adsorbed in CFLPF1, as evidenced by the occurrence of a distinct band at

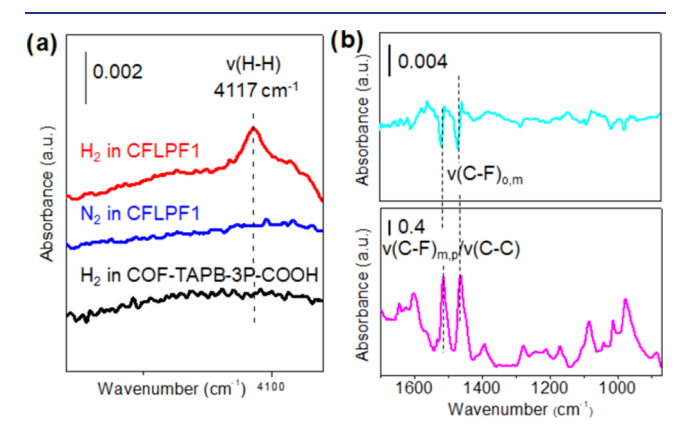


Figure 6. (a) Difference spectra showing exposure of CFLPF1 to H_2 and N_2 , and COF-TAPB-3P-COOH to H_2 at ~20 bar, 25 °C. Each spectrum is referenced to the activated (empty) sample. (b) Difference spectrum in the 1800–800 cm⁻¹ region after exposure of CFLPF1 to H_2 (top) and IR absorbance spectrum of empty CFLPF1 (bottom). Notations and acronyms: ν , stretch; ortho, o; meta, m; para, p.

4117 cm⁻¹ that can be attributed to the H-H stretching vibration (ν). Compared with the value of gas phase ortho- H_2 at 4155 cm^{-1,21a} ν (H–H) in CFLPF1 displays a redshift of 38 cm⁻¹, falling into the range of 35-45 cm⁻¹ indicating bond weakening due to interaction between H2 and functional groups. ^{21b} The assignment of 4117 cm⁻¹ to adsorbed H₂, most likely bound to CFLP, is further confirmed by measuring the CFLPF1 sample after exposure to N2, which does not show a peak in this region, and by the observation that it is also absent in the H₂-exposed pristine COF-TAPB-3P-COOH sample (see Figure 6a). Examination of the lower frequency region (1700– 800 cm⁻¹) in the difference spectrum reveals that upon loading H_2 , the absorption bands associated with stretching of C-C/C-F bonds at different positions of $B(C_6F_5)_3^{21c}$ are primarily perturbed, as typified by the derivative-like features (see Figure 6b), which provides further evidence that H2 mainly interacts with CFLP groups. We further disclosed the underlying mechanism of activation/dissociation of H2 by the CFLPF catalyst under real reaction conditions. The change on the wet sample (dispersing CFLPF1 in toluene solvent) before and after exposure to H₂ at 60 bar was tracked through attenuated total reflection (ATR) IR. The differential spectrum of H₂exposed CFLPF1 in Figure S25 showed a broad absorption band in the region 3300-3000 cm⁻¹. This feature is most likely due to $\nu(N-H)$ stretching. An evident band at a low wavenumber of 1254 cm⁻¹ and a small yet noticeable gain around 2350 cm⁻¹ correspond to bending and stretching vibrations of B-H, respectively. All of these spectral features serve as direct evidence of the formation of N-H and B-H due to H2 dissociation. More remarkably, after the addition of the substrate methyl 2-phenyl acrylate, clear loss of these bands except bending $\beta(B-H)$ that is marked by the absorption bands of the added reactant was observed, which points to the consumption of dissociated H2 species by reacting with the substrate. Meanwhile, XPS measurements revealed B 1s binding energy shifts to a lower value in solution-derived CFLPF1-H₂ relative to the pristine CFLPF1 (Figure S26), consistent with heterolytic activation of H₂ in solution.²²

Furthermore, we carried out hydrogenation using D_2 in place of H_2 to measure the kinetic isotope effect (KIE) and reveal the dynamic process of hydrogenation (Figure S27). We found that the reaction rate decreased slightly giving a normal $K_{\rm H}/K_{\rm D}$ of $1.2^{23{\rm a}}$ because of the zero-point energy difference between isotopic isomers. The near-unity of the KIE indicates that cleavage of the $H_2(D_2)$ bond occurs simultaneously with the formation of the B-H(D) and N-H(D) bonds in a concerted mechanism. $^{23{\rm b}}$ This implies that the rate-determining step of hydrogen activation may be $H_2(D_2)$ diffusion to the active FLP sites rather than the $H_2(D_2)$ cleavage.

Computational insight into the catalytic mechanism is provided by the Gibbs energy profile of the reaction pathway, calculated with R1HNCOCH₃ + B(C_6F_5)₃ and R1NH₂ + B(C_6F_5)₃ serving as models for CFLPF1 and its homogeneous counterpart, respectively (Figure 7 and Figures S28, S30, and S31, see details in the Supporting Information). As expected, the experimental results in which CFLPF1 exhibited an enhanced yield and enantioselectivity were supported by the calculated results. Two pathways were considered: a "proton-first" pathway (blue in Figure 7, Figure S28) in which a proton is transferred to the substrate at the β -position of the olefin and a "hydride-first" pathway (red in Figure 7, Figure S28) in which a hydride is transferred to the substrate at the β -position of the olefin. Attempts to transfer the proton or hydride to the

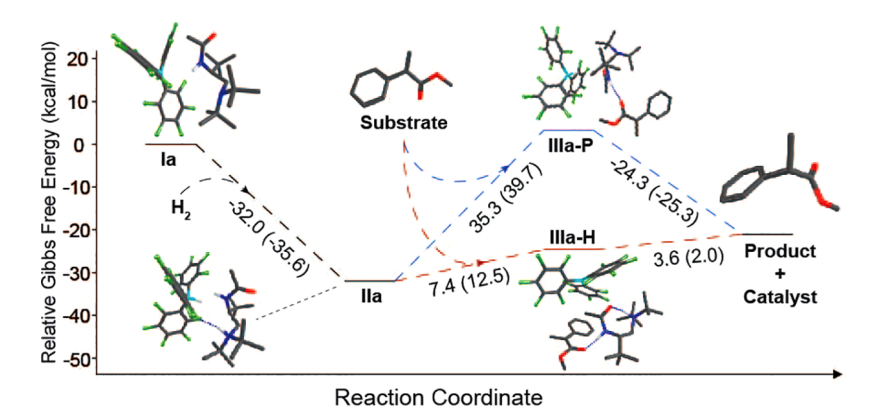


Figure 7. Calculated Gibbs free energies (gas phase) of CFLPF1 with R1*HNCOCH $_3$ + B(C $_6$ F $_5$) $_3$ as the model for H $_2$ activation and subsequent olefin hydrogenation at B3LYP/LANL2DZ/D3 level (Red = O, Blue = N, Green = F, Light blue = B, Gray = C, White = H). Energy values between parentheses were calculated using toluene as the solvent.

 α -position resulted in spontaneous rearrangement, resulting in a proton or hydride transfer to the β -position. A preference for the "hydride-first" pathway is observed in both systems; however, the thermodynamic difference between the pathways is greater in the CFLPF1 model. Specifically, the CFLPF1 model predicts a ΔG difference between the proton-first intermediate and the hydride-first intermediate of 27.9 kcal/ mol (IIIa, Figure 7), whereas the homogeneous system model predicts a ΔG difference of 17.7 kcal/mol (IIIb, Figure S28). Catalyst-to-substrate chirality transfer is favored by the "hydride-first" pathway because only the Lewis base is chiral. Therefore, the transfer of a proton from the protonated chiral Lewis base to the hydride addition intermediate as the second step can be expected to have significantly increased enantioselectivity. Chirality transfer in these systems requires hydrogen bonding, as evidenced by CFLPF2 reactivity within the same scope of esters as CFLPF1. Specifically, only when CFLPF2 was exposed to a substrate with a H-bonding donor moiety, 1-phenyl 1-aminomethylethene, chirality transfer was observed as a consequence of hydrogen bonding interaction between the oxazoline/ester backbone linkage of the chiral Lewis base and the amine. Additionally, when the reaction of was performed in a THF solvent that can competitively inhibit hydrogen bonding of substrate, the ee value decreased by 34% (Table 1, Entry 9). Furthermore, the lowest energy structures of the intermediate geometries, regardless of the pathway, reveal the existence of catalyst substrate N-H···O hydrogen bonding from the substrate ester carbonyl oxygen to the amide or amine N-H for IIIa and IIIb, respectively. Careful examination of the FT-IR spectrum of CFLPF1 + 1a displayed a redshift in the C=O stretching vibration $(1641-1655 \text{ cm}^{-1})$ and a blueshift in the N-H bending vibration (1517-1713 cm⁻¹) compared with CFLPF1 (Figure S29), consistent with hydrogen bonding between the two moieties. Since the energy difference between the proton- and the hydride-first pathways is >18 kcal/mol for both catalysts, these results alone do not account for the observed enantioselectivity enhancement.

The importance of hydrogen bonding for product yield and chirality transfer was further explored in silico. Specifically, the protic N-H of the protonated Lewis base is stabilized by the amide-oxygen hydrogen bonding interaction, leaving the amide N-H readily accessible to hydrogen bonding with the substrate. Hydride addition products bind to this site in one of two orientations to create reaction pathways generating the S-enantiomer (S-path) or the R-enantiomer (R-path) products.

Transition state calculations of the proton transfer step reveal a reduced transition state barrier energy ($\Delta G = 10.8$ and 16.1 kcal/mol for the S and R paths, respectively) for the CFLPF1 model relative to the homogeneous model ($\Delta G = 18.5$ and 19.9 kcal/mol for the S and R paths, respectively), due to the stronger hydrogen bonding interaction of the amide nitrogen with the ester carbonyl of the substrate (Figures S30 and S31). The reduced energy of the proton transfer transition state is consistent with the increased product yield of CFLPF1 under identical conditions as the homogeneous analogue. The enhanced enantioselectivity was found to originate in the disparate thermodynamics of intermediates along the R- and Soriented pathways (Figure S30) due to the presence of a stable intermediate with a pair of H bonds between (1) the substrate ether carbonyl and the protic amine and (2) another H-bond between the ester oxygen and the amide N-H, a configuration inaccessible for the substrate on the R path. Additionally, a lower energy-bound product configuration exists for the R path $(\Delta G = -2.4 \text{ kcal/mol relative to the S-path analogue}),$ resulting in an increased thermodynamic barrier for product release relative to the S path. The combination of the 3.3 kcal/ mol higher proton transfer barrier and more sluggish product release leads to the enhanced enantioselectivity observed in CFLPF1, and the absence of a H-bond donor moiety in CFLPF2 explains the lack of enantioselectivity within the same substrate scope.

CONCLUSIONS

In summary, a transformative combination of the rationally designed COF with newly developed CFLPs via postmodification has generated a class of versatile CFLPF catalysts. They feature both a metal-free and recyclable nature and exhibit impressive catalysis performance in asymmetric hydrogenation of olefins. By inheriting the crystallinity and porosity of COF, CFLPF can serve as an efficient nanoreactor within which the enrichment of catalytically active CFLP promotes H₂ activation. The heterogeneous CFLPF was demonstrated to be more thermodynamically favorable relative to the corresponding homogeneous CFLP because of the postmodification-induced stabilization of transition states. Calculations clearly support that the enforced chiral environment boosts the enantioselectivity under the regulation of hydrogen bonding by differentiating the intermediates of the stereospecific pathways. This work not only contributes CFLPF as a new catalyst platform but also paves the way for achieving

asymmetric catalysis and beyond based on catalyst advancement via a judicious combination of porous materials with CFLP.

ASSOCIATED CONTENT

Supporting Information

The Supporting Information is available free of charge at https://pubs.acs.org/doi/10.1021/jacs.3c11607.

PXRD curves, BET tests, SEM and mapping images for structural determination and examination, FT-IR and XPS spectra for compositional investigation, CD and VCD spectra for an optical property survey, HPLC and NMR results for performance determination, experimental materials and methods, as well as calculation details (PDF)

AUTHOR INFORMATION

Corresponding Author

Shengqian Ma — Department of Chemistry, University of North Texas, Denton, Texas 76201, United States; orcid.org/0000-0002-1897-7069; Email: shengqian.ma@unt.edu

Authors

Yin Zhang — Department of Chemistry, University of North Texas, Denton, Texas 76201, United States; orcid.org/ 0000-0002-6066-0495

Jun Guo – State Key Laboratory of Separation Membranes and Membrane Processes, School of Chemistry, Tiangong University, Tianjin 300387, China; orcid.org/0000-0001-6277-3947

Peter VanNatta – Department of Chemistry, University of North Texas, Denton, Texas 76201, United States

Yao Jiang — School of Chemistry and Chemical Engineering, Hefei University of Technology, Hefei 230009, China; orcid.org/0000-0002-2316-8274

Joshua Phipps – Department of Chemistry, University of North Texas, Denton, Texas 76201, United States

Roknuzzaman Roknuzzaman – Department of Chemistry, University of North Texas, Denton, Texas 76201, United States

Hassan Rabaâ — Department of Chemistry, University of North Texas, Denton, Texas 76201, United States; Department of Chemistry, Ibn Tofail University, ESCTM, Kenitra 14000, Morocco; orcid.org/0000-0002-6901-0608

Kui Tan – Department of Chemistry, University of North Texas, Denton, Texas 76201, United States

Thamraa AlShahrani – Department of Physics, College of Science, Princess Nourah bint Abdulrahman University, Riyadh 11564, Saudi Arabia

Complete contact information is available at: https://pubs.acs.org/10.1021/jacs.3c11607

Author Contributions

[#]Y.Z. and J.G. contributed equally.

Notes

The authors declare no competing financial interest.

ACKNOWLEDGMENTS

The authors thank the support from the Robert A. Welch Foundation (B-0027). The authors also extend their

appreciation to the Deanship of Scientific Research at Princess Nourah Bint Abdulrahman University for partially funding this work through the Visiting Researcher Program. The authors are thankful for computational resources funded by NSF grant OAC-2117247 supporting CRUNTCH4. Jun Guo thanks the financial support from the National Natural Science Foundation of China (No. 22103055).

REFERENCES

- (1) (a) Cui, X.; Burgess, K. Catalytic Homogeneous Asymmetric Hydrogenations of Largely Unfunctionalized Alkenes. *Chem. Rev.* **2005**, *105*, 3272–3296. (b) Kraft, S.; Ryan, K.; Kargbo, R. B. Recent Advances in Asymmetric Hydrogenation of Tetrasubstituted Olefins. *J. Am. Chem. Soc.* **2017**, *139*, 11630–11641. (c) Verendel, J. J.; Pàmies, O.; Diéguez, M.; Andersson, P. G. Asymmetric Hydrogenation of Olefins Using Chiral Crabtree-type Catalysts: Scope and Limitations. *Chem. Rev.* **2014**, *114*, 2130–2169. (d) Massaro, L.; Zheng, J.; Margarita, C.; Andersson, P. G. Enantioconvergent and Enantiodivergent Catalytic Hydrogenation of Isomeric Olefins. *Chem. Soc. Rev.* **2020**, *49*, 2504–2522.
- (2) (a) Knowles, W. S. Asymmetric Hydrogenations (Nobel Lecture). Angew. Chem., Int. Ed. 2002, 41, 1998–2007. (b) Noyori, R. Asymmetric Catalysis: Science and Opportunities (Nobel Lecture). Angew. Chem., Int. Ed. 2002, 41, 2008–2022. (c) Li, W.; Schlepphorst, C.; Daniliiuc, C.; Glorius, F. Asymmetric Hydrogenation of Vinylthioethers: Access to Optically Active 1,5-Benzothiazepine Derivatives. Angew. Chem., Int. Ed. 2016, 55, 3300–3303. (d) Chen, Q.-A.; Ye, Z.-S.; Duan, Y.; Zhou, Y.-G. Homogeneous Palladium-catalyzed Asymmetric Hydrogenation. Chem. Soc. Rev. 2013, 42, 497–511. (e) Roseblade, S. J.; Pfaltz, A. Iridium-Catalyzed Asymmetric Hydrogenation of Olefins. Acc. Chem. Res. 2007, 40, 1402–1411.
- (3) (a) Halterman, R. L.; Vollhardt, K. P. C.; Welker, M. E.; Blaeser, D.; Boese, R. Designed, Enantiomerically Pure, Fused Cyclopentadienyl Ligand with C₂ Symmetry: Synthesis and Use in Enantioselective Titanocene-Catalyzed Hydrogenations of Alkenes. J. Am. Chem. Soc. 1987, 109, 8105–8107. (b) Chirik, P. J. Iron- and Cobalt-Catalyzed Alkene Hydrogenation: Catalysis with Both Redox-Active and Strong Field Ligands. Acc. Chem. Res. 2015, 48, 1687–1695. (c) Wen, J.; Wang, F.; Zhang, X. Asymmetric Hydrogenation Catalyzed by First-row Transition Metal Complexes. Chem. Soc. Rev. 2021, 50, 3211–3237.
- (4) Knowles, W. S.; Sabacky, M. J. Catalytic Asymmetric Hydrogenation employing a Soluble, Optically Active, Rhodium Complex. *Chem. Commun.* **1968**, 1445–1446.
- (5) Miyashita, A.; Yasuda, A.; Takaya, H.; Toriumi, K.; Ito, T.; Souchi, T.; Noyori, R. Synthesis of 2,2′-Bis(diphenylphosphino)-1,1′-binaphthyl (BINAP), an Atropisomeric Chiral Bis(triaryl)phosphine, and Its Use in the Rhodium(I)-Catalyzed Asymmetric Hydrogenation of α -(Acylamino)acrylic Acids. *J. Am. Chem. Soc.* **1980**, *102*, 7932–7934.
- (6) (a) Zhu, S.-F.; Zhou, Q.-L. Iridium-Catalyzed Asymmetric Hydrogenation of Unsaturated Carboxylic Acids. *Acc. Chem. Res.* **2017**, *50*, 988–1001. (b) Reetz, M. T.; Meiswinkel, A.; Mehler, G.; Angermund, K.; Graf, M.; Thiel, W.; Mynott, R.; Blackmond, D. G. Why Are BINOL-Based Monophosphites Such Efficient Ligands in Rh-Catalyzed Asymmetric Olefin Hydrogenation? *J. Am. Chem. Soc.* **2005**, *127* (29), 10305–10313.
- (7) (a) Huang, Y.; Walji, A. M.; Larsen, C. H.; MacMillan, D. W. C. Enantioselective Organo-Cascade Catalysis. *J. Am. Chem. Soc.* **2005**, 127, 15051–15053. (b) Ouellet, S. G.; Tuttle, J. B.; MacMillan, D. W. C. Enantioselective Organocatalytic Hydride Reduction. *J. Am. Chem. Soc.* **2005**, 127, 32–33. (c) Yang, J. W.; Hechavarria Fonseca, M. T.; Vignola, N.; List, B. Metal-Free, Organocatalytic Asymmetric Transfer Hydrogenation of α , β -Unsaturated Aldehydes. *Angew. Chem., Int. Ed.* **2005**, 44, 108–110. (d) Mayer, S.; List, B. Asymmetric Counteranion-Directed Catalysis. *Angew. Chem., Int. Ed.* **2006**, 45, 4193–4195.

- (8) (a) Blaser, H.-U.; Malan, C.; Pugin, B.; Spindler, F.; Steiner, H.; Studer, M. Selective Hydrogenation for Fine Chemicals: Recent Trends and New Developments. *Adv. Synth. Catal.* **2003**, 345, 103–151. (b) Stoffels, M. A.; Klauck, F. J. R.; Hamadi, T.; Glorius, F.; Leker, J. Technology Trends of Catalysts in Hydrogenation Reactions: A Patent Landscape Analysis. *Adv. Synth. Catal.* **2020**, 362, 1258–1274.
- (9) (a) Stephan, D. W.; Erker, G. Frustrated Lewis Pairs: Metal-free Hydrogen Activation and More. *Angew. Chem., Int. Ed.* **2010**, 49, 46–76. (b) Paradies, J. Metal-Free Hydrogenation of Unsaturated Hydrocarbons Employing Molecular Hydrogen. *Angew. Chem., Int. Ed.* **2014**, 53, 3552–3557.
- (10) (a) Stephan, D. W.; Erker, G. Frustrated Lewis Pair Chemistry of Carbon, Nitrogen and Sulfur Oxides. Chem. Sci. 2014, 5, 2625–2641. (b) Stephan, D. W. Frustrated Lewis Pairs: From Concept to Catalysis. Acc. Chem. Res. 2015, 48, 306–316. (c) Stephan, D. W. The Broadening Reach of Frustrated Lewis Pair Chemistry. Science 2016, 354, No. aaf7229. (d) Liu, L. L.; Stephan, D. W. Radicals Derived from Lewis Acid/Base Pairs. Chem. Soc. Rev. 2019, 48, 3454–3463. (e) Jupp, A. R.; Stephan, D. W. New Directions for Frustrated Lewis Pair Chemistry. Trends Chem. 2019, 1, 35–48. (f) Lam, J.; Szkop, K.; Mosaferi, E.; Stephan, D. W. FLP Catalysis: Main Group Hydrogenations of Organic Unsaturated Substrates. Chem. Soc. Rev. 2019, 48, 3592–3612. (g) Stephan, D. W. Catalysis, FLPs, and Beyond. Chem. 2020, 6, 1520–1526. (h) Stephan, D. W. Diverse Uses of the Reaction of Frustrated Lewis Pair (FLP) with Hydrogen. J. Am. Chem. Soc. 2021, 143, 20002–20014.
- (11) (a) Feng, X.; Du, H. Metal-free Asymmetric Hydrogenation and Hydrosilylation Catalyzed by Frustrated Lewis Pairs. *Tetrahedron Lett.* **2014**, *55*, 6959–6964. (b) Liu, Y.; Du, H. Frustrated Lewis Pair Catalyzed Asymmetric Hydrogenation. *Acta Chim. Sinica.* **2014**, *72*, 771–777. (c) Shi, L.; Zhou, Y. Enantioselective Metal-Free Hydrogenation Catalyzed by Chiral Frustrated Lewis Pairs. *ChemCatChem.* **2015**, *7*, 54–56. (d) Meng, W.; Feng, X.; Du, H. Frustrated Lewis Pairs Catalyzed Asymmetric Metal-Free Hydrogenations and Hydrosilylations. *Acc. Chem. Res.* **2018**, *51*, 191–201. (e) Dai, Y.; Meng, W.; Feng, X.; Du, H. Chiral FLP-catalyzed Asymmetric Hydrogenation of 3-Fluorinated Chromones. *Chem. Commun.* **2022**, *58*, 1558–1560.
- (12) (a) Rueping, M.; Sugiono, E.; Steck, A.; Theissmann, T. Synthesis and Application of Polymer-Supported Chiral Brønsted Acid Organocatalysts. *Adv. Synth. Catal.* **2010**, 352, 281–287. (b) Han, X.; Yuan, C.; Hou, B.; Liu, L.; Li, H.; Liu, Y.; Cui, Y. Chiral Covalent Organic Frameworks: Design, Synthesis and Property. *Chem. Soc. Rev.* **2020**, 49, 6248–6272. (c) Kang, X.; Stephens, E. R.; Spector-Watts, B. M.; Li, Z.; Liu, Y.; Liu, L.; Cui, Y. Challenges and Opportunities for Chiral Covalent Organic Frameworks. *Chem. Sci.* **2022**, 13, 9811–9832.
- (13) (a) Dioos, B. M. L.; Vankelecom, I. F. J.; Jacobs, P. A. Aspects of Immobilisation of Catalysts on Polymeric Supports. *Adv. Synth. Catal.* **2006**, 348, 1413–1446. (b) He, Y.-M.; Nobile, C. F.; He, Y.-M.; Feng, Y.; Fan, Q.-H. Asymmetric Hydrogenation in the Core of Dendrimers. *Acc. Chem. Res.* **2014**, 47, 2894–2906. (c) Sun, Q.; Dai, Z.; Meng, X.; Xiao, F.-S. Homochiral Porous Framework as a Platform for Durability Enhancement of Molecular Catalysts. *Chem. Mater.* **2017**, 29, 5720–5726. (d) Grabovskii, S. A.; Akchurin, T. I.; Dokichev, V. A. Heterogeneous Palladium Catalysts in the Hydrogenation of the Carbon-carbon Double Bond. *Curr. Org. Chem.* **2021**, 25, 315–329. (e) Wang, X.; Li, J.; Lu, S.; Liu, Y.; Li, C. Efficient Enantioselective Hydrogenation of Quinolines Catalyzed by Conjugated Microporous Polymers with Embedded Chiral BINAP Ligand. *Chin. J. Catal.* **2015**, 36, 1170–1174.
- (14) (a) Geng, K. Y.; He, T.; Liu, R. Y.; Dalapati, S.; Tan, K. T.; Li, Z. P.; Tao, S. S.; Gong, Y. F.; Jiang, Q. H.; Jiang, D. L. Covalent Organic Frameworks: Design, Synthesis, and Functions. *Chem. Rev.* 2020, 120, 8814–8933. (b) Li, Z. E.; He, T.; Gong, Y. F.; Jiang, D. L. Covalent Organic Frameworks: Pore Design and Interface Engineering. *Acc. Chem. Res.* 2020, 53, 1672–1685. (c) Ding, S.-Y.; Wang, W. Covalent Organic Frameworks (COFs): from Design to Applications.

- Chem. Soc. Rev. 2013, 42, 548–568. (d) Zhang, T.; Zhang, G.; Chen, L. 2D Conjugated Covalent Organic Frameworks: Defined Synthesis and Tailor-Made Functions. Acc. Chem. Res. 2022, 55 (6), 795–808. (e) Zhang, P. H.; Wang, Z. F.; Cheng, P.; Chen, Y.; Zhang, Z. J. Covalent-Organic-Framework-Based Composite Materials. Coordin. Chem. Rev. 2021, 438, No. 213873. (f) Liu, Y.; Zhou, W. Q.; Teo, W. L.; Wang, K.; Zhang, L. Y.; Zeng, Y. F.; Zhao, Y. L. Design and Application of Ionic Covalent Organic Frameworks. Chem 2020, 6, 3172–3202.
- (15) Gao, B.; Feng, X.; Meng, W.; Du, H. Asymmetric Hydrogenation of Ketones and Enones with Chiral Lewis Base Derived Frustrated Lewis Pairs. Angew. Chem., Int. Ed. 2020, 59, 4498–4504. (16) (a) Zhang, Y.; Lan, P.; Martin, K.; Ma, S. Porous Frustrated Lewis Pair Catalysts: Advances and Perspective. Chem. Catal. 2022, 2, 439–457. (b) Niu, Z.; Gunatilleke, W.; Sun, Q.; Lan, P.; Perman, J.; Ma, J.-G.; Cheng, Y.; Aguila, B.; Ma, S. Metal-Organic Framework Anchored with a Lewis Pair as a New Paradigm for Catalysis. Chem 2018, 4, 2587–2599. (c) Niu, Z.; Zhang, W.; Lan, P.; Aguila, B.; Ma, S. Promoting Frustrated Lewis Pairs for Heterogeneous Chemoselective Hydrogenation via the Tailored Pore Environment within Metal-Organic Frameworks. Angew. Chem., Int. Ed. 2019, 58, 7420–7424.
- (17) Vasko, P.; Fuentes, M. Á.; Hicks, J.; Aldridge, S. Reversible O-H Bond Activation by an Intramolecular Frustrated Lewis Pair. *Dalton Trans.* **2019**, *48*, 2896–2899.
- (18) Zhang, Y.; Chen, S. B.; Al-Enizi, A. M.; Nafady, A.; Tang, Z. Y.; Ma, S. Q. Chiral Frustrated Lewis Pair@Metal-Organic Framework as a New Platform for Heterogeneous Asymmetric Hydrogenation. *Angew. Chem.*, 2023, 135, No. e202213399.
- (19) (a) Pietruszka, J.; Schölzel, M. Ene Reductase-Catalysed Synthesis of (R)-Profen Derivatives. *Adv. Synth. Catal.* **2012**, *354*, 751–756. (b) Classen, T.; Pietruszka, J.; Schuback, S. M. Revisiting the Enantioselective Sequence Patterns in Enoate Reductases. *ChemCatChem* **2013**, *5*, 711–713.
- (20) (a) Scott, D. J.; Fuchter, M. J.; Ashley, A. E. Metal-Free Hydrogenation Catalyzed by an Air-Stable Borane: Use of Solvent as a Frustrated Lewis Base. *Angew. Chem., Int. Ed.* **2014**, *53*, 10218–10222. (b) Gyömöre, Á.; Bakos, M.; Földes, T.; Pápai, I.; Domján, A.; Soós, T. Moisture-Tolerant Frustrated Lewis Pair Catalyst for Hydrogenation of Aldehydes and Ketones. *ACS Catal.* **2015**, *5*, 5366–5372.
- (21) (a) Nijem, N.; Veyan, J. F.; Kong, L.; Wu, H.; Zhao, Y.; Li, J.; Langreth, D. C.; Chabal, Y. J. Molecular Hydrogen "Pairing" Interaction in a Metal Organic Framework System with Unsaturated Metel Centers (Mof-74). J. Am. Chem. Soc. 2010, 132, 14834–14848. (b) Hadjiivanov, K. I.; Panayotov, D. A.; Mihaylov, M. Y.; Ivanova, E. Z.; Chakarova, K. K.; Andonova, S. M.; Drenchev, N. L. Power of Infrared and Raman Spectroscopies to Characterize Metal-Organic Frameworks and Investigate Their Interaction with Guest Molecules. Chem. Rev. 2021, 121, 1286–1424. (c) Marques, L. R.; Ando, R. A. Infrared Spectroscopy Evidence of Weak Interactions in Frustrated Lewis Pairs Formed by Tris(Pentafluorophenyl)Borane. ChemPhysChem 2023, 24, No. e202200715.
- (22) (a) Geier, S. J.; Stephan, D. Lutidine/B(C_6F_5)₃: At the Boundary of Classical and Frustrated Lewis Pair Reactivity. *J. Am. Chem. Soc.* **2009**, *131*, 3476–3477. (b) Willms, A.; Schumacher, H.; Tabassum, T.; Qi, L.; Scott, S.; Hausoul, P.; Rose, M. Solid Molecular Frustrated Lewis Pairs in a Polyamine Organic Framework for the Catalytic Metal-free Hydrogenation of Alkenes. *ChemCatChem* **2018**, *10*, 1835–1843. (c) Scott, D. J.; Fuchter, M.; Ashley, A. Metal-Free Hydrogenation Catalyzed by an Air-Stable Borane: Use of Solvent as a Frustrated Lewis Base. *Angew. Chem., Int. Ed.* **2014**, *53*, 10218–10222.
- (23) (a) Houghton, A. Y.; Autrey, T. Calorimetric Study of the Activation of Hydrogen by Tris(pentafluorophenyl)borane and Trimesitylphosphine. *J. Phys. Chem. A* **2017**, *121*, 8785–8790. (b) Schulz, F.; Sumerin, V.; Heikkinen, S.; Pedersen, B.; Wang, C.; Atsumi, M.; Leskelä, M.; Repo, T.; Pyykkö, P.; Petry, W.; Rieger, B. Molecular Hydrogen Tweezers: Structure and Mechanisms by

Neutron Diffraction, NMR, and Deuterium Labeling Studies in Solid and Solution. *J. Am. Chem. Soc.* **2011**, *133*, 20245–20257.